A ^{224}Ra-labeled polyoxopalladate as putative radiopharmaceutical

Gott, M.; Yang, P.; Kortz, U.; Stephan, H.; Pietzsch, H.-J.; Mamat, C.;

Originally published:

June 2019

Chemical Communications 55(2019), 7631-7634

DOI: https://doi.org/10.1039/C9CC02587A

Journal Name

COMMUNICATION

A ^{224}Ra-labeled polyoxopalladate as putative radiopharmaceutical

Matthew Gott,[a]† Peng Yang,[b] Ulrich Kortz,*[b] Holger Stephan,*[a] Hans-Jürgen Pietzsch,[a] and Constantin Mamat*[a]

Received 00th January 20xx,
Accepted 00th January 20xx

DOI: 10.1039/x0xx00000x

www.rsc.org/

Abstract. Despite its attractive properties, internal targeted alpha therapies using $^{223/224}$Ra are limited to bone-seeking applications. As there is no suitable chelator available, the search for new carriers to stably bind Ra^{2+} and to connect it to biological target molecules is necessary. Polyoxopalladates represent a class of compounds where Ra^{2+} can be easily introduced into the Pd-POM core during a facile one-pot preparation. Due to the formation of a protein corona, the connection to other targeting (bio)macromolecules is possible.

Radiotherapy approaches using alpha-emitting radionuclides show great promise for treating oncologic diseases and several recent reviews provide in-depth information on the results of these studies.[1-3] Alpha-emitting radionuclides are significantly more efficient at inducing cell death than the more widely used beta-emitters (1-5 α-particles versus 3000-6000 β-particles) due to their significantly higher linear energy transfer (100 keV·µm^{-1} versus 0.2 keV·µm^{-1}).[4] Therefore there is of great interest for alpha-emitting radiopharmaceuticals. Current clinical research is focused on a number of radionuclides such as ^{211}At, $^{212/213}$Bi, $^{223/224}$Ra,[5] and ^{225}Ac.[6] The radium isotopes are currently the most widely available and therefore were the focus of this research.[7-9]

Radium has two radiopharmaceutical relevant radioisotopes, ^{223}Ra ($t_{1/2}$ = 11.43 d; 5.176 MeV α) and ^{224}Ra ($t_{1/2}$ = 3.63 d; E_α = 5.685 MeV). Both isotopes eject four α particles and two β$^-$-particles before ending as stable lead isotopes, ^{207}Pb and ^{208}Pb, respectively.[10] Due to the ultra-short penetration range of α-particles, both decay series deliver a massive dose of ionizing radiation (approx. 27-28 MeV) over a short range (50-100 µm). The large size of α-particle radiation results in a high probability of inducing double-strand DNA breaks,[11] resulting in a potent cytotoxic effect in the targeted cancer cells which ultimately results in cell death.[4] The appropriate half-lives of these radionuclides would increase their use in radioimmunotherapy applications with antibodies and peptides.

Meanwhile, [^{223}Ra]$RaCl_2$ has become the first α-emitting radiopharmaceutical to be FDA and EMA approved for clinical applications (Xofigo®).[8,12,13] The clinical approval of this radionuclide leads to possible incorporation into novel therapeutic radiopharmaceuticals. However, the difficulty of forming an in-vivo-stable chelator system has hindered the development of radium-based radiotherapeutic drugs so far. Due to radium's highly basic character and preferential Ra^{2+} ionic formation in aqueous environments, chelation has mostly focused on macrocyclic ligands. Several hydrophilic chelators such as DOTA, DTPA, and Kryptofix 2.2.2 as well as the more hydrophobic calix[4]arene derivatives were tested in the past.[14-17] Due to the difficult stabilization of Ra^{2+} in a chelating agent, several groups made attempts to encapsulate Ra^{2+} in nanocarriers[18,19] like functionalized nanozeolites[20] or liposomes,[21,22] for a stable in-vivo-transport of this ion. Good binding of Ra^{2+} was observed, but release and accumulation of ^{223}Ra on bone surfaces still occurred. Additionally, it was noted by de Kruijff et al. that they did not report if equilibrium had been reached, and the stability may be greatly altered out of equilibrium.[1] From the existing body of research, it has been demonstrated that stabilization of the Ra^{2+} necessitates a high degree of "encapsulation" such as the stabilizing basket of a calix crown complex or incorporation into the matrix of a nanoparticle. In this work, we evaluate a novel and facile approach using palladium-based polyoxometallates (POMs) to stably incorporate ^{133}Ba and ^{224}Ra as central ions.

Polyoxopalladates (Pd-POMs) represent a noble metal-based subset of polyoxometallates.[23,24] In respect of bioactivity, POMs have been demonstrated to exhibit antitumor, antiviral, and even antiretroviral characteristics.[25-27] Recently, Yang et al. demonstrated a family of molecular polyoxopalladate hosts encapsulating alkaline earth metal guests (Ca^{2+}, Sr^{2+}, and Ba^{2+}).[28]

[a] *Helmholtz-Zentrum Dresden-Rossendorf, Institute of Radiopharmaceutical Cancer Research, Dresden, Germany. Email: h.stephan@hzdr.de; c.mamat@hzdr.de*
[b] *Jacobs University, Department of Life Sciences and Chemistry, Bremen, Germany. E-mail: u.kortz@jacobs-university.de*
† *current address: Argonne National Laboratory, Physics Division, Lemont, Illinois, USA.*

Electronic Supplementary Information (ESI) available: purification of the Pd-POMs, radiolabelling procedures, analyses of radio-TLCs. See DOI: 10.1039/x0xx00000x

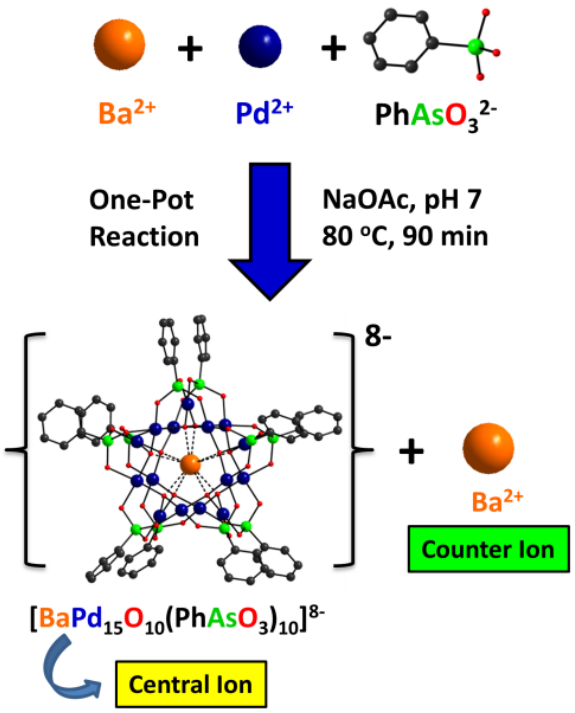

Scheme 1. Synthetic route for the facile one-pot preparation of ^{133}Ba- and ^{224}Ra-labeled polyoxopalladates.

This quick one-pot reaction provides alkaline-earth-metal-centered, phenylarsonate-capped Pd-POMs that bear high stability in aqueous media within a large pH window (5 to 8). Moreover, a further functionalization of the phenylarsonate capping group could enable the attachment of targeting molecules.[29] With this in mind, initial studies were performed to determine the applicability of such polyoxopalladates as carrier in targeted alpha therapy to develop a stable "host-guest" system for radium. The $BaPd_{15}$ system was chosen to incorporate the radionuclides ^{224}Ra as well as ^{133}Ba as a surrogate for radium. During the synthesis, the polyanion is formed with barium both as central and counter ions (Scheme1).

A critical step in the synthetic procedure is the complete removal of radionuclides bound outside. The simple, one-pot synthesis of $[BaPd_{15}O_{10}(PhAsO_3)_{10}]^{8-}$ polyanion is based on a previously published method by Kortz and colleagues.[28] The resulting $Na_xBa_y[BaPd_{15}O_{10}(PhAsO_3)_{10}]$ (**Na_xBa_y-BaPd$_{15}$**) (with x + 2y = 8) is well water-soluble and exhibits its best stability close to a physiological pH. Radiolabeled preparations were accomplished the same way with an addition of $[^{133}Ba]BaCl_2$ (or $[^{224}Ra]RaCl_2$) prior to heating the sample.

The crude **Na_xBa_y-BaPd$_{15}$** is achieved in a sodium acetate buffer and contained an excess of different dissolved ions. Various methods were used to purify this product (Scheme 2) including precipitation and chromatographic separations. It is important, especially for the radiolabeled products, to remove the free ^{133}Ba or ^{224}Ra. For precipitation, several ammonium salts (see ESI) were tested with freshly prepared **Na_xBa_y-BaPd$_{15}$**, but only guanidinium chloride precipitated. Tests were performed to determine the quantity of extracted **Gua-BaPd$_{15}$** and the removal of dissolved ions. Aliquots of **Na_xBa_y-BaPd$_{15}$** were combined with excess guanidinium chloride to form the precipitate **Gua-BaPd$_{15}$**. After being serial washed with acetonitrile, centrifuged and dried, a recovery of **Gua-BaPd$_{15}$** in 94% was determined. These samples were dissolved in DMSO and analyzed by ICP-MS to examine the product purity. Interestingly, ICP-MS showed the presence of excess Ba^{2+}. It was believed that Ba^{2+} was likely trapped during the precipitation of **Gua-BaPd$_{15}$** and was not completely removed during the serial washing step or there was externally bound barium that remained attached to the $[BaPd_{15}O_{10}(PhAsO_3)_{10}]^{8-}$ polyanion. For this reason, column chromatography methods were evaluated to quickly remove the unwanted, unbound Ba^{2+} in solution and determine the amount of externally bound Ba^{2+}.

Size exclusion chromatography was tested to isolate the large polyanion from the significantly smaller starting materials (e.g. Ba^{2+} and OAc^-). Due to the difference in size, the polyanion would be expected to pass off the Sephadex G-15 (MWCO = 1000 Da) column quickly in a tight band with the void volume, while the smaller molecules would be retained by the resin. In practice, the colored Pd-POM product was eluted in a major band at the solvent front (ESI Figure 6). Some tailing was noted and a portion of the material remained trapped at the top of the column. The presence of **Na_xBa_y-BaPd$_{15}$** was confirmed by ^{1}H and ^{13}C NMR. However, the separation was found to be ineffective as a significant excess of acetate was still observed in the ^{13}C NMR spectrum (ESI Figure S2). From labeling experiments, approx. 45.4% of the activity were determined, indicating that $[^{133}Ba]Ba^{2+}$ was still bound to the **[^{133}Ba]Ba$_x$-Pd$_{15}$** (theoretical value: 28.3%). Thus, not all of the free Ba^{2+} was retained on the column.

Cation exchange chromatography was further tested to remove the unbound Ba^{2+}. A column with Dowex-50 resin (Na^+ form) was loaded with the crude product mixture and extracted with H_2O. The Pd-POM was easily followed on the column due to its orange- brown color and only colored fractions were collected from the column to avoid sample dilution. ICP-MS studies, utilizing the Ba/Pd ratio, showed a large reduction in external excess of Ba^{2+}. The initial crude mixture contains a Ba/$BaPd_{15}$ ratio of approx. 4.5/1 while the purified sample **Na-BaPd$_{15}$** contains a Ba/$BaPd_{15}$ ratio of 1.5/1.

The ^{133}Ba-containing sample **[^{133}Ba]Na-BaPd$_{15}$** was purified under the same conditions. Assuming the extraction of Ba^{2+} by this method is highly efficient, the final activity in the separated sample should represent 28.3% of bound ^{133}Ba. Experimentally,

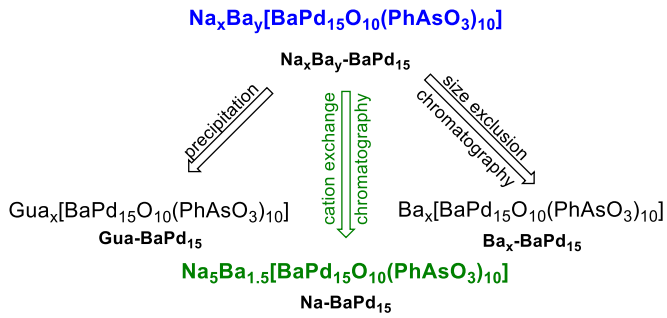

Scheme 2. Procedures used for the purification of the radiolabeled **[^{133}Ba/^{224}Ra]Na-Ba(Ra)Pd$_{15}$** and the non-labeled **Na-BaPd$_{15}$**.

approx. 30% of the activity related to the [^{133}Ba]**Na-BaPd$_{15}$** is found. The results (see ESI Table S2) are consistent with the expected bound barium. At this current stage, this method will be utilized for future labeling experiments with ^{133}Ba and ^{224}Ra to remove the unbound cations, which is the primary concern for radiopharmaceutical applications.

Next, a simple dialysis study was performed to analyze the stability of [^{133}Ba]**Na-BaPd$_{15}$** in an aqueous environment and evaluate the release of the externally bound Ba^{2+}. An aliquot of Dowex-purified [^{133}Ba]**Na-BaPd$_{15}$**-solution was added to a pre-conditioned Pur-A-Lyzer Midi 1000 dialysis tubes (MWCO = 1000). As the dialysis was performed, fractions of the dialysis water were collected at various time points and the ^{133}Ba-activity determined using a NaI detector. Any activity observed was assumed to be unbound [^{133}Ba]Ba^{2+} as barium bound to [^{133}Ba]**Na-BaPd$_{15}$** could not pass through the membrane. After a period of 96 hours, the rate of diffusion tapered off and only 12.5% of the [^{133}Ba]Ba^{2+} had diffused (Figure 1, ESI Table S3). With the ICP-MS data showing that roughly a third of the barium is externally bound, this outcome is significantly lower than expected. Therefore, the ionic interaction between the Pd-POM and the Ba^{2+} appears quite strong.

To distinguish between non-radiolabeled Ba^{2+} and **Na-BaPd$_{15}$** as well as between the radiolabeled [^{133}Ba]Ba^{2+} and [^{133}Ba]**Na-BaPd$_{15}$**, a TLC method was developed to separate the barium cation and the resulting $BaPd_{15}$-POM. The difficulty was to detect Ba^{2+} as it is uncolored and UV inactive. Thus, it was decided to follow the colored **Na-BaPd$_{15}$**. Reverse phase TLC (RP-18) was used due to the high charge of the polyanion. Different solvent systems were tested (ESI Table S1) and the best result was observed with a water/acetonitrile mixture (ratio: 1/2) as eluent. Afterwards, the method was tested with radiolabeled [^{133}Ba]**Na-BaPd$_{15}$** and [^{133}Ba]Ba^{2+}, because both species are now detectable at the radio-TLC. The evaluation of the radio-TLC shows the mobility of the [^{133}Ba]**Na-BaPd$_{15}$** with the solvent front as expected and confirms that [^{133}Ba]Ba^{2+} stays at the origin (Figure 2/ESI Figure S3). Using this method, a clear distinction between the two species is possible.

For further in vitro and in vivo tests, cation-exchange separated [^{133}Ba]**Na-BaPd$_{15}$** was incubated with freshly prepared rat serum to evaluate the interaction with serum proteins. The uncontacted Pd-POM acted as expected with the colored spot visibly moving with the solvent front and unbound [^{133}Ba]Ba^{2+}

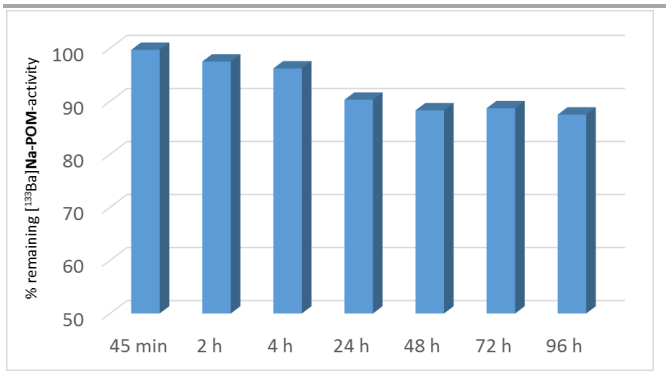

Figure 1. Dialysis results examining the stability of the radiolabeled [^{133}Ba]**Na-BaPd$_{15}$** over a period of 96 hours.

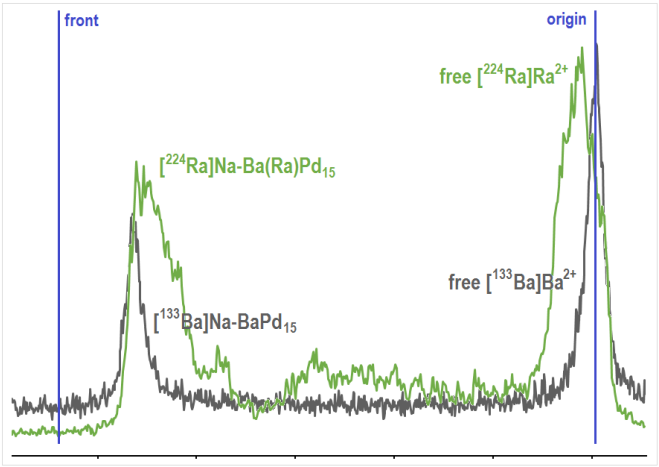

Figure 2. Radio-TLC's showing the [^{133}Ba]**Na-BaPd$_{15}$** (gray) and the [^{224}Ra]**Na-Ba(Ra)Pd$_{15}$** (green) immediately after preparation with an R_f = 0.9 and the free [^{133}Ba]Ba^{2+}/[^{224}Ra]Ra^{2+} staying at the origin.

remaining at the origin (ESI Figure S7). However, the Pd-POM contacted with rat serum exhibited a distinctly different behavior. The colored spot was observed to move with the solvent front initially, but once the spot lost contact with the solvent front, it no longer migrated and thus barely moved from the origin (ESI Figure S8 & Table S4). A further test was performed to eliminate issues with the protein interaction on the TLC plate. Methanol was added to the [^{133}Ba]**Na-BaPd$_{15}$**-serum-mixture for denaturation and it was centrifuged to isolate the proteins. Interestingly, the protein pellet at the bottom contained the entire colored product and the supernatant was clear. The formation of a protein corona around the highly charged [^{133}Ba]**Na-BaPd$_{15}$** is the reason for this behavior. It is well known that due to their size, shape and negative charge, Pd-POMs form aggregates with positively charged domains of proteins, which are stabilized by electrostatic interactions and hydrogen bonds.[30,31] Of further interest, there was no activity found in the supernatant of the denatured protein. Although it was visibly clear that the colored product remained with the protein pellet, it was expected to see unbound [^{133}Ba]Ba^{2+} originating from the externally bound Ba^{2+} suggesting that the interaction was strong enough to trap free barium within the protein corona.

The radium-containing [^{224}Ra]**Na-Ba(Ra)Pd$_{15}$** was synthesized following the same one-pot-method described vide supra. Cation exchange chromatography was used to remove any unbound [^{224}Ra]Ra^{2+}. Samples of the unreacted radium

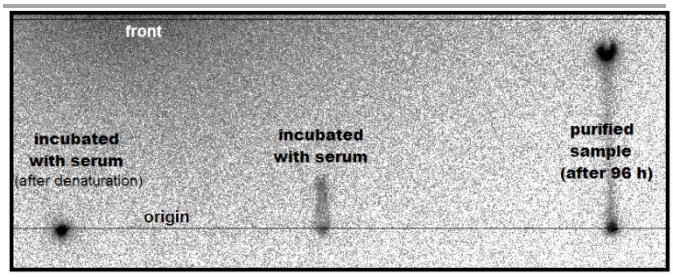

Figure 3. Radiographic image of TLC plates containing [^{133}Ba]Ba^{2+} with intact serum proteins (left), [^{133}Ba]**Na-BaPd$_{15}$** with intact serum proteins (middle), and uncontacted [^{133}Ba]**Na-BaPd$_{15}$** (right) after 96 h.

solution and purified Pd-POM were analyzed using the alpha spectrometry to understand the relative ratios ^{224}Ra and its daughters ^{212}Pb and ^{212}Bi inferring their uptake in the product (ESI Figure S4). The relative ratios of radium and its daughters are not significantly changed from the starting ^{224}Ra-solution to the [^{224}Ra]**Na-Ba(Ra)Pd$_{15}$** product. This suggests that the insertion is not selective for radium. Thus, lead- and bismuth-centered Pd-POMs are likely also produced.

To further establish that ^{224}Ra was actually incorporated into the Pd-POM core and not just the daughters, a radio-TLC was performed to demonstrate that the radioactivity moves with the POM. A large activity amount moves with the front as expected for the [^{224}Ra]**Na-Ba(Ra)Pd$_{15}$** (ESI Figure S5). Streaking of the Pd-POM product is noted in this chromatogram, but this could be related to the different metals incorporated into the final [^{224}Ra]**Na-Ba(Ra)Pd$_{15}$**. The radio-TLC was left for 1 week to decay and reimaged, which ensures that the only remaining activity results from ^{224}Ra and not only from the daughters. Though the signal is significantly weakened, the chromatogram confirms that radium-224 was incorporated into [^{224}Ra]**Na-Ba(Ra)Pd$_{15}$** and not just the daughters.

To conclude, the polyanion $[BaPd_{15}O_{10}(PhAsO_3)_{10}]^{8-}$ radiolabeled with ^{133}Ba and ^{224}Ra to yield [^{133}Ba]**Na-BaPd$_{15}$** and [^{224}Ra]**Na-Ba(Ra)Pd$_{15}$** have been demonstrated for the first time. An effective cation exchange method was utilized to remove unbound ions (e.g. $^{nat}Ba^{2+}$, [^{133}Ba]Ba^{2+} and [^{224}Ra]Ra^{2+}) from the resulting Pd-POM. ICP-MS studies demonstrated that a portion of the unincorporated M^{2+} remains to the polyanion surface, but strongly externally bound. Studies using rat serum indicated a high affinity of the radiolabeled Pd-POMs to serum proteins to form a persistent corona. Importantly, this protein corona seemingly retains the Pd-POM and also its externally bound cations. Targeting approaches with specific proteins such as antibodies and their fragments is possible due to the formation of these radiolabeled protein-POM-aggregates. In-vivo-stability experiments will be necessary in the future to further determine the viability of these radiolabelled Pd-POM derivatives for radiopharmaceutical applications.

Conflicts of interest

There are no conflicts to declare.

Notes and references

§ Ulrich Kortz acknowledges the German Science Foundation (DFG, KO-2288/20-1, KO-2288/16-1) and Jacobs University for research support. Peng Yang thanks the China Scholarship Council (CSC) for a doctoral fellowship.

1 R.M. de Kruijff, H.T. Wolterbeek and A.G. Denkova, *Pharmaceuticals*, 2015, **8**, 321.
2 J. Kozempel, O. Mokhodoeva and M. Vlk, *Molecules,* 2018, **23**, 581.
3 S.V. Gudkov, N.Y. Shiyagina, V.A. Vodeneev and A.V. Zvyagin, *Int. J. Mol. Sci.*, 2016, **17**, 33.
4 B.M. Kim, Y. Hong, S. Lee, P. Liu, J.H. Lim, Y.H. Lee, T.H. Lee, K.T. Chang and Y. Hong, *Int. J. Mol. Sci.,* 2015, **16**, 26880-26913.
5 E. Etchebehere, A.E. Brito , A. Rezaee, W. Langsteger and M. Beheshti, *Eur. J. Nucl. Med. Mol. Imaging*, 2017, **44**(Suppl 1), 84.
6 A. Morgenstern, C. Apostolidis, C. Kratochwil, M. Sathekge, L. Krolicki and F. Bruchertseifer, *Curr. Radiopharm.*, 2018, **11**, 200.
7 T.J. Wadas, D.N. Pandya, K.K. Solingapuram Sai and A. Mintz, *AJR Am. J. Roentgenol.*, 2014, **203**, 253.
8 H. Jadvar and D.I. Quinn, *Clin. Nucl. Med.*, 2013, **38**, 966.
9 M. Picciotto, T. Franchina, A. Russo, G.R.R. Ricciardi, G. Provazza, S. Sava, S. Baldari, O. Caffo and V. Adamo V., *Expert Opin. Pharmacother.,* 2017, **18**, 899.
10 M. Gott, J. Steinbach and C. Mamat, *Open Chem.*, 2016, **14**, 118.
11 J.P. Pouget, I. Navarro-Teulon, M. Bardiès, N. Chouin, G. Cartron, A. Pèlegrin and D. Azria, *Nat. Rev. Clin. Oncol.* 2011, **8**, 720.
12 O.S. Bruland, T.J. Jonasdottir, D.R. Fisher and R.H. Larsen, *Curr. Radiopharm.,* 2008, **1**, 203.
13 G. Vaidyanathan and M.R. Zalutsky, *Curr. Radiopharm.* 2011, **4**, 283.
14 G. Henriksen, P. Hoff and R.H. Larsen, *Appl. Radiat. Isot.*, 2002, **56**, 667.
15 X. Chen, M. Ji and D.R. Fisher, C.M. Wai, *Inorg. Chem*., 2009, **38**, 5449.
16 D. Bauer, M. Gott, J. Steinbach and C. Mamat, *Spectrochim. Acta A*, 2018, **199**, 50.
17 J. Steinberg, D. Bauer, F. Reissig, M Köckerling, H-J. Pietzsch and C. Mamat, *ChemOpen*, 2018, **7**, 432.
18 J. Kozempel, M. Vlk, E. Málková, A. Bajzíková, J. Bárta, R. Santos-Oliveira and A. Malta Rossi, *J. Radioanal. Nucl. Chem.*, 2014, **304**, 443.
19 F. Reissig, R. Hübner, J. Steinbach, H.-J. Pietzsch and C. Mamat, *Inorg. Chem. Front.*, 2019, **6**, DOI: DOI: 10.1039/C9QI00208A.
20 A. Piotrowska, E. Leszczuzuk, F. Bruchertseifer, A. Morgenstern and A. Bilewicz*, J. Nanoparticle Res.*, 2013, **15**, 2082.
21 T.J. Jonasdottir, D.R. Fisher, J. Borrebaek, O.S. Bruland and R.H. Larsen, *Anticancer Res.*, 2006, **26**, 2841.
22 G. Henriksen, B.W. Schoultz, T.E. Michaelsen, O.S. Bruland and R.H. Larsen, *Nucl. Med. Biol.*, 2013, **31**, 441.
23 N.V. Izarova, M.T. Pope and U. Kortz, Angew. Chem. Int. Ed., 2012, 51, 9492.
24 P. Yang and U. Kortz, *Acc. Chem. Res.*, 2018, **51**, 1599.
25 M.T. Pope and A. Müller, *Angew. Chem. Int. Ed.*, 1991, **30**, 34.
26 J. Rhule, C. Hill, D. Judd and R.F. Schinazi, *Chem. Rev.*, 1998, **98**, 327.
27 S.-Y. Lee, A. Fiene, W. Li, T. Hank, K. Brylev, V.E. Fedorov, J. Lecka, A. Haider, H.-J. Pietzsch, H. Zimmermann, J. Sévigny, U. Kortz, H. Stephan and C.E. Müller, *Biochem. Pharmacol*. 2015, **93**, 171.
28 P. Yang, Y. Xiang, Z. Lin, B.S. Bassil, J. Cao, L. Fan, Y. Fan, M.-X. Li, P. Jiménez-Lozano, J.J. Carbó, J.M. Poblet and U. Kortz, *Angew. Chem. Int. Ed.*, 2014, **53**, 11974.
29 P. Yang, H. Li, T. Ma, F. Haso, T. Liu, L. Fan, Z. Lin, C. Hu and U. Kortz, *Chem. Eur. J.*, 2018, **24**, 2466.
30 M. Arefian, M. Mirzaei, H. Eshtiagh-Hosseini and A. Frontera, *Dalton Trans.*, 2017, **46**, 6812.
31 A. Bijelic and A. Rompel, *Coordination Chem. Rev.,* 2015, **299**, 22.

